Theor Chem Acc (2000) 103:469–476
DOI 10.1007/s002149900080

Theoretical
Chemistry Accounts

Regular article

Energetics, structures, bonding, and kinetics of the HSCl–HClS system

Fernando R. Ornellas

Instituto de Química, Universidade de São Paulo, Caixa Postal 26077, São Paulo, SP, 05599-970, Brazil

Received: 7 May 1999 / Accepted: 22 July 1999 / Published online: 4 October 1999

Abstract. The [H,S,Cl] potential-energy surface has been investigated at the self-consistent field (SCF), complete active space self-consistent field (CASSCF), second-order Møller–Plesset, coupled-cluster single-double and perturbative triple excitation, [CCSD(T)]/6-31G(d,p), 6-31G(2df,2pd), and correlation-consistent polarized valence triple zeta (cc-pVTZ) levels of theory. CCSD(T)/cc-pVTZ results predict a very stable HSCl species, an isomer HClS, 51.84 kcal/mol higher in energy, and a transition state 57.68 kcal/mol above HSCl. Independent of the level of theory, results with the smaller 6-31G(d,p) basis set turned out to be poor, especially for HClS. Vibrational analysis indicates that both species can be easily differentiated if isolated. Bonding differences between these molecules are illustrated by contour plots of valence orbitals. Viewed classically, bonding in HClS involves a dative bond. Transition-state rate constants, and equilibrium constants for the HSCl ↔ HClS isomerization have been estimated for various temperatures (200–1000 K). At 298.15 K, the forward rate is predicted to be 7.95×10^{-29} s^{-1}, and the equilibrium constant to be 2.31×10^{-38}. Tunneling corrections vary from 1.57 at 298.15 K to 1.05 at 1000 K. Activation energies have been obtained by a two-points linear fit to the Arrhenius equation.

Key words: Thiohypochlorous acid – Isomerization – Bonding – Thermochemistry – Rate constant

1 Introduction

The characterization of species containing both sulfur and chlorine atoms of potential relevance for the modeling of chemical reactions occurring in the atmosphere is of importance for scientists involved in understanding their reaction cycles [1]. Motivated by indications that reactive chlorine can be released from sea salt and, therefore, that suitable conditions might be found in the remote marine boundary layer for the formation of sulfur–chlorine compounds, where the surfaces of aerosol particles may play a catalytic role, Eberhard et al. [2] recently carried out a series of experiments involving the $Cl/Cl_2/H_2S$ reaction system. In their investigation, a discharge-flow reactor with a photoionization mass spectrometer, having a synchrotron as a source of radiation, was used to measure the photoionization efficiency spectra, and also the ionization energies of the species produced in the reaction. Complementing the experimental work, results for the geometry and ionization potential determined by ab initio calculations within the G2 method have also been reported for the sulfur species detected in that study. Geometries were optimized at the Hartree–Fock (HF)/6-31G(d) and second-order Møller–Plesset (MP2)(full)/6-31G(d) levels of theory. Ionization energies were computed at the MP4 and quadratic configuration interaction with singles doubles (QCISD)(T,E4T) levels of theory using more extended basis sets, but employing the MP2(full)/6-31G(d) optimized geometries. HSCl was one of the species detected in that work, but no reference was made to its isomer HClS.

In this study, we are mainly concerned with a more systematic characterization of the [H,Cl,S] potential-energy surface (PES) by ascertaining the effects of increasingly higher levels of correlation treatment, complete active space self-consistent field (CASSCF), MP2, coupled-cluster with all single and double excitations and connected triples [CCSD(T)], and basis sets, 6-31G(d,p), 6-31G(2df,2pd), correlation-consistent polarized valence triple zeta (cc-pVTZ) on the structural parameters, frequencies, and relative energies of the isomeric species. The differences in bonding between the two molecules are also discussed. The transition state for the HSCl ↔ HClS isomerization reaction is also determined, and the rates for both forward and reverse reactions are computed as a function of temperature, as well as the equilibrium constant. An intrinsic reaction path calculation nicely confirms this transition state as the proper first-order saddle point connecting the two isomers. Besides providing more accurate results for the HSCl species, and characterizing for the first time the

HClS molecule, it is also our hope that this study can indicate further trends as to the degree of reliability of the different levels of theory, especially with the smaller 6-31G(d) basis set. This point will turn out to be relevant if similar investigations are extended to larger systems containing sulfur and chlorine atoms where high-level calculations can become quite expensive. Additionally, considering the reliability of the results of this investigation, we expect it can guide experimentalists in the search of the as yet unknown species characterized here.

2 Method

Basically, three different structures were investigated: the angular isomers HSCl and HClS, and a kind of cyclic structure SHCl, which would be expected to correspond to a transition state connecting the two isomers. All calculations started at the HF level, and subsequently the effects of electron correlation on the structures, frequencies, energetics, bonding, and consequently on the kinetics of all three species were incorporated into the calculation through MP2 perturbation theory, and by the CCSD(T) technique, as implemented in the Gaussian 94 series of programs [3]. Core electrons were kept frozen for all correlated calculations. Static correlation was also estimated by taking into account the distribution of 14 valence electrons into nine valence orbitals in a multiconfiguration SCF calculation. This procedure essentially corresponds to a valence-shell CASSCF approach. The nature of all stationary points was examined through the calculation of vibrational frequencies in the harmonic oscillator approximation. Three standard basis sets were employed in the expansion of the molecular orbitals: the 6-31G(d,p) and 6-31G(2df,2pd) developed by Pople and coworkers [4] and the cc-pVTZ set of Dunning [5]. We recall that, as originally developed, five and seven components were employed for the d- and f-type functions, respectively, of the cc-pVTZ set.

Chemical dynamics calculations were performed within the framework of conventional transition-state theory (TST) [6]. For a canonical ensemble, the TST rate constant for a unimolecular reaction involving singlet species is given by

$$k_{\alpha}^{TST}(T) = (k_B T/h)[q^{\#}(T)/q_{\alpha})] \exp\{-\Delta E^{\#}/k_B T\} \ ,$$

where k_B is Boltzmann's constant, h is Planck's constant, $q^{\#}(T)$ and q_{α} are the partition functions for the transition-state species and the reactant, with $\alpha = f$ or $\alpha = r$ for the forward or the reverse reactions, respectively. Energies were measured relative to the bottom of the PES of the most stable species, HSCl. A multiplicative correction term to account for quantum mechanical tunneling was estimated using Wigners' approach [7], and is expressed as

$$\Gamma = 1 + (1/24)[h\omega/k_B T]^2 \ ,$$

where ω stands for the absolute value of the imaginary frequency at the first-order saddle point. Partition functions were computed with the Gaussian suite of programs. Arrhenius activation energies were evaluated by a two-points fit of the rate constant at two different temperatures, and the equilibrium constants were obtained as the ratio of both forward and reverse rate constants.

3 Results and discussion

3.1 Structural and vibrational analysis

Let us first consider some general points that are quite independent of basis sets and methods of calculation. Only two minima were found on the PES, with the global one corresponding to the isomer HSCl. Based on the data in Tables 1 and 2, one can immediately infer that for any combination of method/basis set, both the SCl bond length and the bond angle in HSCl are significantly different than in HClS. In HClS, the bond angle is found to be about 9° larger than in HSCl, and the SCl distance longer by about 0.1–0.2 Å for the correlated results. Within a method, all calculations with the smaller basis set [6-31G(d,p)] predict the SCl bond length to be systematically larger in both compounds, whereas with the 6-31G(2df,2pd) basis it is found to be systematically smaller, but closer to the results with the cc-pVTZ set. In the case of the HS bond length, it is found to be relatively invariant to basis sets and methods, with most results differing in the third decimal place, with the exception of the CASSCF lengths, which are longer by about 0.01–0.02 Å. As to the HCl distance, within a method it changes only slightly with the basis sets, but within the correlated methods the distances can differ by as much as 0.015 Å. Notice also that the inclusion of just static correlation results in an overestimated value not only for the SCl internuclear distance, but also for the HS and HCl bond lengths, a trend which is expected for this type of calculation.

Concerning the adequacy of the 6-31G(d,p) basis set, one can notice that calculations with different methods yielded an SCl internuclear distance in HSCl within 1–2% of the results obtained with the more extended sets;

Table 1. Optimized geometric parameters (Å, degrees) and harmonic frequencies (cm^{-1}) for the isomer HSCl using various methods and basis sets. Intensities (km/mol) are given in *parentheses*

Method	Basis set	SCl length	SH length	HSCl angle	ω_1	ω_2	ω_3
SCF	6-31G(d,p)	2.034	1.326	96.61	576 (22.62)	1030 (6.86)	2903 (2.43)
	6-31G(2df,2pd)	2.027	1.328	96.50	584 (21.69)	1014 (3.52)	2856 (0.06)
	cc-pVTZ	2.032	1.329	96.32	578 (21.10)	1009 (2.05)	2854 (0.09)
MP2	6-31G(d,p)	2.047	1.333	96.09	542 (12.04)	964 (5.45)	2819 (3.82)
	6-31G(2df,2pd)	2.033	1.336	95.67	565 (13.14)	940 (2.13)	2766 (0.29)
	cc-pVTZ	2.038	1.338	95.50	555 (12.59)	928 (1.15)	2752 (0.14)
CASSCF	6-31G(d,p)	2.091	1.354	96.09	478	925	2622
	6-31G(2df,2pd)	2.074	1.354	96.19	507	915	2588
	cc-pVTZ	2.080	1.356	96.03	500	909	2582
CCSD(T)	6-31G(d,p)	2.066	1.338	95.86	510	944	2753
	6-31G(2df,2pd)	2.051	1.340	95.51	539	922	2714
	cc-pVTZ	2.056	1.343	95.33	529	911	2696

Table 2. Optimized geometric parameters (Å, degrees) and harmonic frequencies (cm^{-1}) for the isomer HClS using various methods and basis sets. Intensities (km/mol) are given in *parentheses*

Method	Basis set	SCl length	HCl length	HClS angle	ω_1	ω_2	ω_3
SCF	6-31G(d,p)	2.357	1.270	101.34	205 (39.55)	607 (15.57)	3141 (93.16)
	6-31G(2df,2pd)	2.202	1.273	102.53	295 (21.06)	692 (4.90)	3062 (101.05)
	cc-pVTZ	2.217	1.274	101.84	290 (21.98)	680 (7.41)	3071 (106.59)
MP2	6-31G(d,p)	2.197	1.280	104.25	311 (19.21)	688 (4.14)	3003 (52.34)
	6-31G(2df,2pd)	2.088	1.289	105.13	412 (0.61)	741 (5.64)	2875 (54.31)
	cc-pVTZ	2.104	1.290	104.05	398 (1.20)	719 (2.29)	2877 (64.32)
CASSCF	6-31G(d,p)	2.315	1.295	101.77	228	604	2853
	6-31G(2df,2pd)	2.202	1.300	103.00	268	646	2776
	cc-pVTZ	2.199	1.301	102.94	229	631	2773
CCSD(T)	6-31G(d,p)	2.263	1.283	103.91	250	631	2953
	6-31G(2df,2pd)	2.136	1.291	104.62	359	691	2840
	cc-pVTZ	2.153	1.291	103.55	348	669	2844

Table 3. Optimized geometric parameters (Å, degrees) and harmonic frequencies (cm^{-1}) for the transition state of the system [H,Cl,S] using various methods and basis sets

Method	Basis set	SCl length	HCl length	HS length	HSCl angle	HClS angle	ω_1	ω_2	ω_3
SCF	6-31G(d,p)	2.341	1.396	1.667	36.05	44.65	345	1145*i*	1951
	6-31G(2df,2pd)	2.303	1.373	1.731	36.44	48.47	336	998*i*	2126
	cc-pVTZ	2.306	1.379	1.725	36.53	48.13	340	1016*i*	2096
MP2	6-31G(d,p)	2.301	1.311	1.981	34.67	59.26	307	887*i*	2642
	6-31G(2df,2pd)	2.204	1.313	2.022	35.87	64.46	391	900*i*	2673
	cc-pVTZ	2.213	1.317	2.017	35.91	63.94	388	886*i*	2637
CASSCF	6-31G(d,p)	2.409	1.349	1.941	34.03	53.63	256	859*i*	2257
	6-31G(2df,2pd)	2.310	1.335	1.995	35.18	59.42	312	806*i*	2440
	cc-pVTZ	2.315	1.340	1.985	35.26	58.78	314	814*i*	2411
CCSD(T)	6-31G(d,p)	2.390	1.320	1.979	33.52	55.88	244	756*i*	2512
	6-31G(2df,2pd)	2.269	1.317	2.028	35.12	62.37	329	769*i*	2609
	cc-pVTZ	2.277	1.322	2.018	35.20	61.63	329	765*i*	2563

however, this is not the case for HClS, where it is found to be longer by about 0.1 Å relative to the results with the other sets. This discrepancy is quite significant and clearly reflects the lack of functions with sufficiently high angular momentum to describe the electron polarization in the formation of a classical dative bond as occurs in HClS and will be discussed in Sect. 3.3.

Based on our best calculation [CCSD(T)/cc-pVTZ], the SCl internuclear distance can be safely estimated to be 2.056 and 2.153 Å, in HSCl and HClS, respectively; the associated bond angles are 95.3 and 103.4°, respectively. Our best prediction for the internuclear distance in the free SCl species turns out to be 2.006 Å (experimentally, 1.975 Å [8]) For the HCl and HS distances in the triatomics, our best results are 1.291 and 1.343 Å, respectively, a result that practically matches the experimental distance (1.346 Å) of the free HS species, and that is sligthly longer than the experimental one for HCl (1.275 Å) [9].

The third stationary point searched for turned out to have a cyclic structure and to correspond to a first-order saddle point. The optimized geometric parameters characterizing this structure and the associated frequencies are collected in Table 3. At our higher level of calculation [CCSD(T)/cc-pVTZ], the SCl internuclear distance turned out to be 2.277 Å, indicating a considerable lengthening relative to the stable isomers. In the transition-state structure, the hydrogen atom is much closer to the chlorine atom (1.322 Å) than to the sulfur one (2.018 Å), leading to an angle of 61.6° for the HClS bond angle; the HSCl angle turned out to be much smaller, 35.2°.

As already pointed out for the case of the stable isomers, independent of the method used, the prediction of geometrical parameters with the smaller basis set differs significantly from the results with the more extended sets, and therefore the analysis of data from calculations with that basis set in larger systems containing both chlorine and sulfur atoms should be carried out bearing in mind the error trends described previously.

Concerning the frequencies, to the best of our knowledge, there are no experimental data available for either isomer, and the results of this study can therefore be taken as a reliable guide to experimentalists in future spectroscopic identification of both species. As to the theoretical predictions, the mode associated with the SCl stretching in HSCl and HClS corresponds to the data under the heading ω_1 in Tables 1 and 2. Our best result yielded 529 cm^{-1} for the SCl harmonic stretching in HSCl, and 348 cm^{-1} in HClS, with the latter value compatible with the longer SCl distance in HClS and indicative of a much flatter PES. For the free SCl molecule, our best theoretical frequency turned out to be 566 cm^{-1}. Based on the MP2 results calculated with the

more extended basis sets, for which vibrational intensities can be estimated, the intensity of the SCl stretching in HSCl is expected to be about 10–20 times that in HClS, in sharp contrast with the prediction evaluated with the 6-31G(d,p) set for which the corresponding intensity in HClS is larger by about 1.6 that in HSCl. In this respect also, this basis set again shows its inadequacy in providing reliable results.

At our highest level of calculation, the vibrational mode ω_3 in Table 1, with a frequency of 2696 cm^{-1}, can be practically associated with the HS stretching, which in the free diatomics was found to be equal to 2692 cm^{-1} at the same level of calculation, and quite close to the experimental value of 2712 cm^{-1}. In the case of the HClS molecule, ω_3 corresponds basically to the HCl stretching with a value of 2844 cm^{-1}; theoretically, ω_e for the free molecule turned out to be 3002 cm^{-1}, whereas experimentally one has 2991 cm^{-1}. This lower value of the HCl stretching frequency in HClS also seems to be indicative of a charge migration away from the HCl internuclear region into the ClS internuclear moiety, thus contributing to the dative bond. This fact is also reflected in the results of a Mulliken population analysis in which the bond polarization Cl^+–S^- is predicted for the HClS molecule with both the SCF and MP2 charge densities. The frequency associated with the bending mode (ω_2) is higher in HSCl (911 cm^{-1}) than in HClS (669 cm^{-1}), indicating a steeper curvature in the PES for this mode in the region of the minimum associated with the HSCl isomer.

3.2 Energetics

Total, relative, and zero-point vibrational energies for all three stationary points are collected in Table 4. As one can clearly see in this table, at all levels of calculation the species HSCl is predicted to be much more stable than HClS. For the correlated calculations, the relative energies determined with the 6-31G(d,p) basis set are approximately 5% larger than those obtained with the two other sets, for which there is a difference of less than about 0.7 kcal/mol between them. Notice also that calculations with the HF method using the two larger sets practically reproduce the results obtained with the CCSD(T) approach, indicating that the contributions of correlation effects at this level to the stabilization of both species seem to be practically identical; however, this is not true for the smaller set, where this energy is overestimated by about 8%. At the MP2 level, the relative energy between the isomers is the largest of all, indicating that the more stable species (HSCl) is favored by the correlation effects introduced at this level. Our best estimate for the location of HClS minimum places it 51.84 kcal/mol above the minimum of the HSCl species.

Concerning the transition state, one can clearly see that correlation effects incorporated through the CCSD(T) method and the larger basis sets lower the energy of the transition state by about 10% relative to the HF results, and by about 4% relative to the MP2 values. This result contrasts with that of the relative energy between the two isomers and is quite significant for the evaluation of the kinetics data since the rate constant depends exponentially on the energy difference between the transition state species and reactants, as discussed in Sect. 3.4. At our highest level of calculation, the transition-state structure lies 57.68 kcal/mol above the minimum of the HSCl molecule.

In order to verify if the first-order saddle point described in Sect. 3.1 does indeed correspond to a transition state connecting the two minima, minimum reaction path calculations within the intrinsic reaction coordinate approach [10], as implemented in the Gaussian suite of programs, were also carried out. The profiles of the energy paths in weighted Cartesian coordinates calculated at the SCF/6-31G(d,p) and MP2/6-31G(2df,2pd) levels are superposed in Fig. 1, and illustrate differences between a correlated approach with an extended set of polarization functions and an SCF calculation with a smaller basis set. For the reverse reaction, in particular, with a smaller barrier, significant errors can be introduced in the calculation of rate constants using the lower-level approach.

For the sake of completeness, we have collected standard thermochemical data for the most stable isomer, HSCl, in Table 5. Heats of formation were estimated using theoretical results at the CCSD(T)/cc-pVTZ level for the reaction

Table 4. Total energies (+857.0 a.u.), relative energies (kcal/mol), and zero-point energies (kcal/mol) in *parentheses* for the stationary states of the system [H,Cl,S] using various methods and basis sets

Method	Basis set	E(HSCl)	E(HClS)	ΔE^{a}_{react}	E(TS)	ΔE^{b}_{TS}
SCF	6-31G(d,p)	−0.553979 (6.45)	−0.473703 (5.65)	50.37	−0.449690 (3.28)	65.44
	6-31G(2df,2pd)	−0.572399 (6.37)	−0.489220 (5.79)	52.19	−0.469194 (3.52)	64.76
	cc-pVTZ	−0.636521 (6.35)	−0.554471 (5.78)	51.49	−0.534513 (3.48)	64.01
MP2	6-31G(d,p)	−0.807467 (6.18)	−0.717998 (5.72)	56.14	−0.705443 (4.21)	64.02
	6-31G(2df,2pd)	−0.916650 (6.10)	−0.830447 (5.76)	54.09	−0.819107 (4.38)	61.21
	cc-pVTZ	−1.002481 (6.25)	−0.917325 (5.71)	53.44	−0.906802 (4.32)	60.04
CASSCF	6-31G(d,p)	−0.594094 (5.75)	−0.509008 (5.27)	53.39	−0.496604 (3.59)	61.18
	6-31G(2df,2pd)	−0.610956 (5.73)	−0.524108 (5.27)	54.50	−0.514880 (3.93)	60.29
	cc-pVTZ	−0.675374 (5.71)	−0.590653 (5.19)	53.16	−0.580580 (3.90)	59.48
CCSD(T)	6-31G(d,p)	−0.845510 (6.01)	−0.758766 (5.48)	54.43	−0.748078 (3.94)	61.14
	6-31G(2df,2pd)	−0.968683 (5.97)	−0.885002 (5.56)	52.51	−0.875103 (4.20)	58.72
	cc-pVTZ	−1.054141 (5.91)	−0.971527 (5.52)	51.84	−0.962226 (4.13)	57.68

[a] $\Delta E_{react} = E(HClS) - E(HSCl)$
[b] $\Delta E_{TS} = E(TS) - E(HSCl)$

$$H_2S + HCl \rightarrow H_2 + HSCl$$

and the experimental heats of formation for both HCl and H_2S [11].

3.3 Bonding

Since geometries optimized at the HF and MP2(full)/6-31G(d) levels of theory for the HSCl isomer and ionization energies calculated with the MP4 and QCISD(T,E4T) methods using more extended basis sets, but employing the MP2(full)/6-31G(d) optimized geometries, are the only theoretical results reported in the literature, to the best of our knowledge, it is worth describing first the basic differences between HSCl and HClS within the framework of the SCF molecular orbital picture.

Making use of a simple visualization in terms of Lewis structures, the bonding in HSCl could certainly be rationalized as resulting from a sharing of the $3p_x$ and $3p_y$ electrons in S and the $1s$ electron in H and the $3p_y$ electron in Cl, with the octet rule obviously satisfied. In the case of HClS, for the octet rule to be satisfied, H and Cl would have to share an electron each, and the Cl atom would contribute with a pair of electrons in a dative-type bond with S. To try to identify elements of this simple picture in the ab initio calculations, we have depicted an orbital energy diagram in Fig. 2, and the orbital densities illustrating the essential differences between the electronic spatial distributions derived from the valence orbitals in Fig. 3. For HSCl, notice that $3a''$ and $4a''$ orbitals are basically the bonding [0.48 $3p_z$(S) + 0.83 $3p_z$(Cl)] and antibonding [0.85 $3p_z$(S) − 0.55 $3p_z$(Cl)] combinations of the atomic $3p_z$ orbitals of S and Cl, respectively. For HClS, these orbitals have a more pronounced atomic character with the chlorine $3p_z$ orbital contributing much less for $4a''$ [0.92 $3p_z$(S) − 0.26

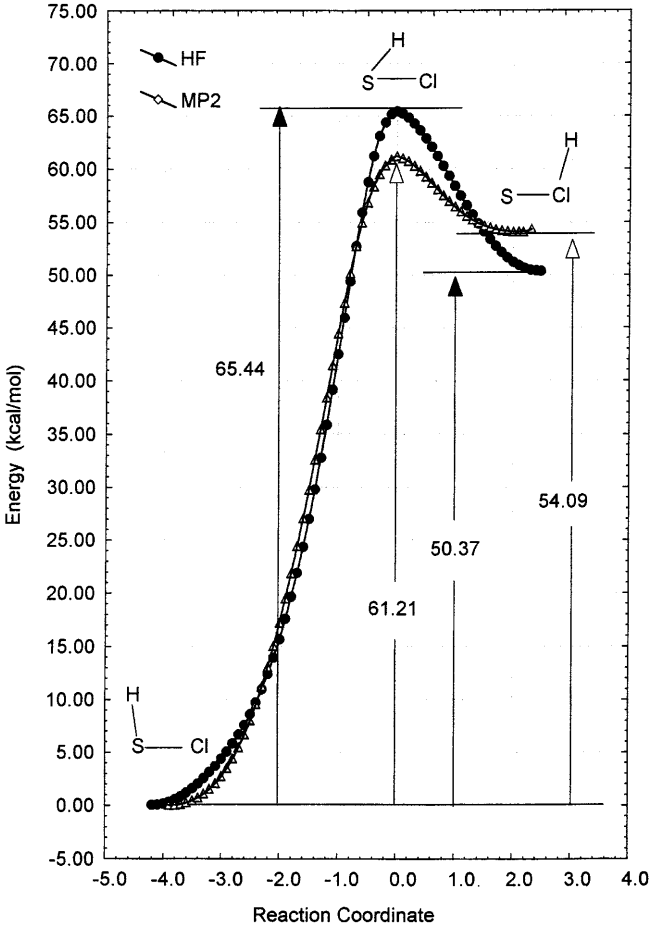

Fig. 1. Energy profiles in terms of the internal reaction coordinate for the HSCl ↔ HClS isomerization reaction at the self-consistent field/6-31G(d,p) and second-order Møller–Plesset (*MP2*) 6-31G(2df,2pd) levels. Energy differences are given in kilocalorie per mole

Table 5. Thermochemical data for HSCl

T (K)	C_p^0 (cal/K mol)	S^0 (cal/K mol)	$H_T^0 - H_0^0$ (kcal/mol)	ΔH_f^0 (kcal/mol)	ΔG_f^0 (kcal/mol)
200	8.74	56.30	1.63	0.83	−1.39
298.15	9.84	59.96	2.53	0.56	−2.45
400	10.31	62.89	3.55	−0.31	−3.41
500	10.80	65.25	4.61	−0.97	−4.10
600	11.18	67.25	5.70	−1.50	−4.68
700	11.49	69.00	6.84	−1.95	−5.17
800	11.76	70.55	8.00	−2.34	−5.60
900	12.00	71.95	9.19	−15.39	−5.73
1000	12.21	73.23	10.40	−15.35	−4.66

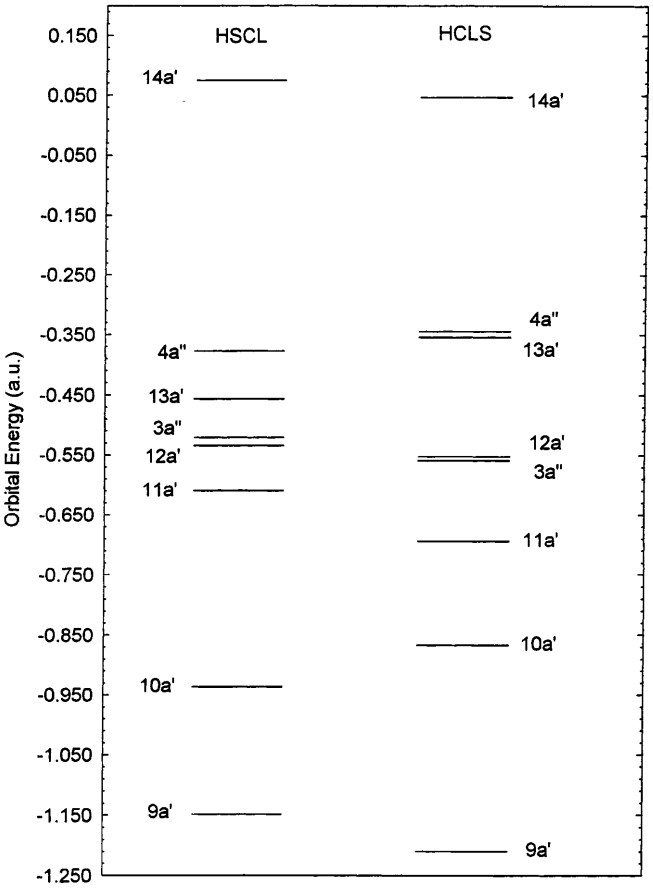

Fig. 2. Valence orbitals energy diagrams for the molecules HSCl and HClS

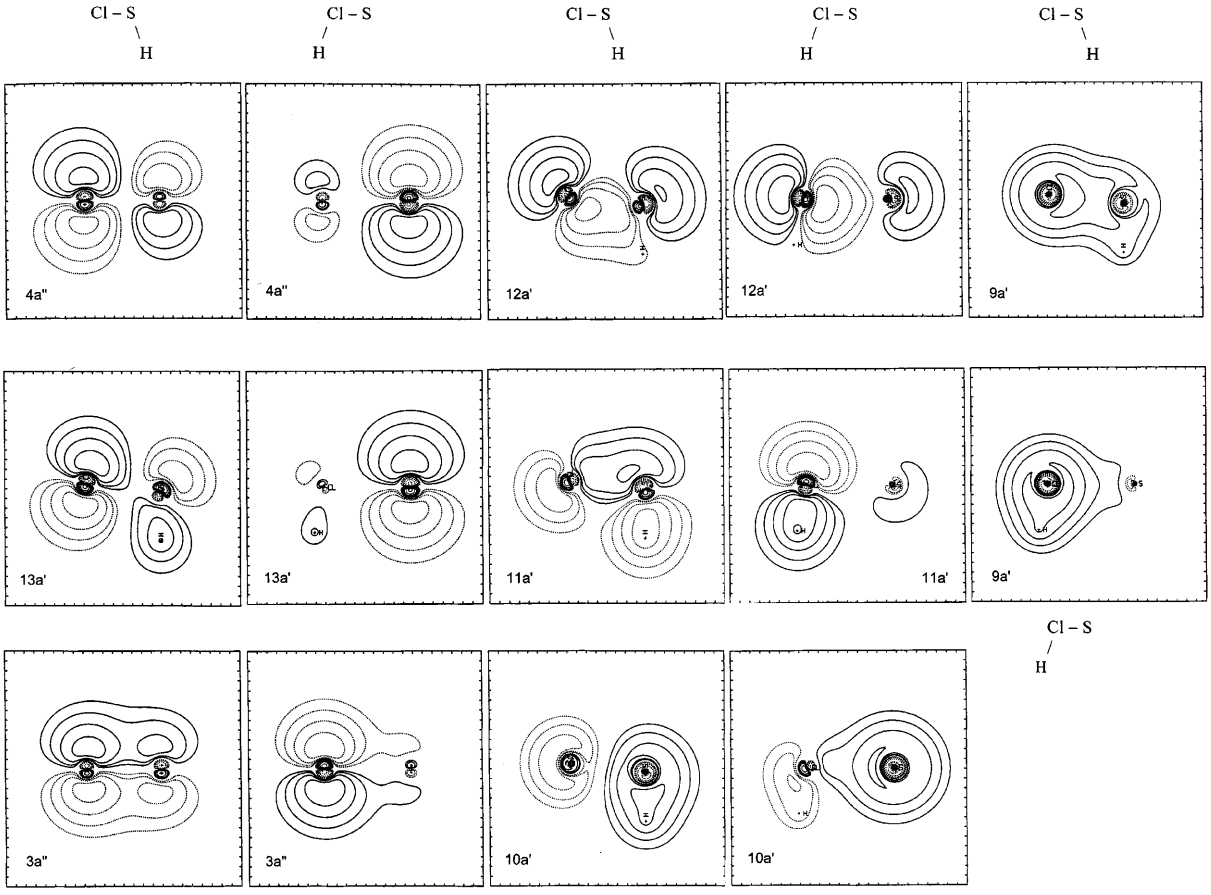

Fig. 3. Cross sections of valence orbitals in the molecular plane (a'), and perpendicular to the molecular plane but containing the SCl internuclear distance (a''). The five contours follow the integrated values of the wavefunctions containing 10, 30, 50, 70, and 90% of the electron density [12]. *Tick marks* are 0.5 a_0 apart. Data for the plots were generated with the MELD program [13]

$3p_z$(Cl)] than in HSCl, and very significantly for $3a''$ [0.18 $3p_z$(S) + 0.98 $3p_z$(Cl)]. It seems clear form these data and Fig. 3 that orbital $3a''$ has a bonding character in HSCl. For HClS, in this simple-minded picture, orbital $4a''$ could essentially be identified with the atomic $3p_z$ orbital of S, and $3a''$ with the $3p_z$ of Cl significantly polarized towards the S atom. This distortion in the charge density is clearly visible in Fig. 3. This same type of distortion can also be noticed for orbital $9a'$, which besides describing a bonding combination between the H and Cl atoms also shows a polarization towards the S atom. The remaining orbitals in HClS are essentially antibonding in character. Notice also that $4a''$ and $13a'$ are almost degenerate, and as clearly shown in Fig. 3, orbital $13a'$ is basically the $3p_x$ orbital of S. The lesser overall build up of charge density between the Cl and S atoms is visible in Fig. 3 for the case of the HClS molecule and somehow reflects the longer SCl internuclear bond length in HClS compared to that in HSCl. Also, as discussed before, we recall that at all levels of calculation the harmonic frequency associated with the SCl stretching was indicative of a much flatter curvature in HClS.

Besides the bonding character of orbital $3a''$ in HSCl, orbitals $10a'$ and $9a'$ also exhibit some bonding features. Orbital $10a'$ which in HClS is essentially the $3s$ of S, becomes locally bonding between the S and H atoms, and orbital $9a'$ shows a bonding delocalization over all the three atoms, despite its major Cl $3s$ contribution. Incidentally, notice that orbital $12a'$ in HSCl shows a slight charge build up between the hydrogen and chlorine atoms.

To try to obtain some numerical estimates of the degree of polarization in the S–Cl moiety, we have collected the gross orbital populations resulting from contributions of the s and p orbitals and the total atomic charges on S and Cl derived from a Mulliken population analysis at the HF/cc-pVTZ level of calculation in Table 6. As seen in this table, these results are clearly indicative of an electron migration towards the S atom in HClS, in contrast with the opposite polarity in HSCl, and this is an element that seems to corroborate the classical picture of a dative bond in HClS.

A description of these molecules at the CASSCF level reveals that for both species the HF configuration is the dominant one with $c_0^2 \sim 0.97$ at their equilibrium internuclear distances. Additionally, application of the T_1 diagnostic as an indicator of non-dynamic correlation results in a value of 0.012, smaller than the threshold of 0.02 recommended by Lee and Taylor [14], values larger than 0.02 indicate an increasing importance of non-dynamical correlation. As to their dipole moments, the

MP2/cc-pVTZ results are 1.41 and 4.03 D for HSCl and HClS, respectively.

3.4 The isomerization reaction

Thermochemical and kinetics data at the standard pressure of 1 atm and various temperatures for the isomerization reaction HSCl → HClS, and for attaining the transition state, calculated at the CCSD(T)/cc-pVTZ level of theory, are collected in Table 7. The energetics data in this table show that the isomerization reaction has a very high forward barrier, slightly above 55 kcal/mol in the temperature range of 200–1000 K. For this unimolecular process, not only is the barrier high, but the species HClS also lies relatively high energetically, making this forward reaction endothermic and non-spontaneous. As to the reverse reaction, HClS → HSCl, one can obviously expect the opposite behavior: a very small barrier (about 4 kcal/mol), an exothermicity of about −52 kcal/mol, and thermodynamic spontaneity, with a change in the Gibbs free energy of about −51 kcal/mol.

As a consequence of the relatively large barrier for the forward reaction, the rate constants change very drastically with temperature; however, despite the variation, the rate for the forward reaction continues to be very small, and once HSCl is formed, it will certainly not undergo isomerization in this range of temperatures. Concerning the reverse reaction, HClS → HSCl, it is so fast that once HClS is formed by any process, it is immediately converted to HSCl. At room temperature, the equilibrium constant for the HSCl → HClS reaction is of the order of 10^{-38}, and at 1000 K it is 10^{-11}. With respect to the Wigner's correction for tunneling, its effect is to increase the rate constant by a

Table 6. Gross orbital populations and total atomic charges on the S and Cl atoms derived from a Mulliken population analysis at the Hartree–Fock/correlation-consistent polarized valence triple zeta level of calculation

	HSCl		HClS	
	S	Cl	Cl	S
$2s + 3s$	3.826	3.944	3.872	3.985
$2p_x + 3p_x$	3.217	3.960	3.329	3.961
$2p_y + 3p_y$	2.804	3.207	3.612	2.332
$2p_z + 3p_z$	3.967	3.972	3.967	3.985
Partial gross populations	13.814	15.083	14.780	14.263
Partial net charges	+0.186	−0.083	+0.220	−0.263
Total atomic charges[a]	+0.020	−0.146	+0.120	−0.321

[a] Includes contributions from the remaining atomic orbitals in the basis set

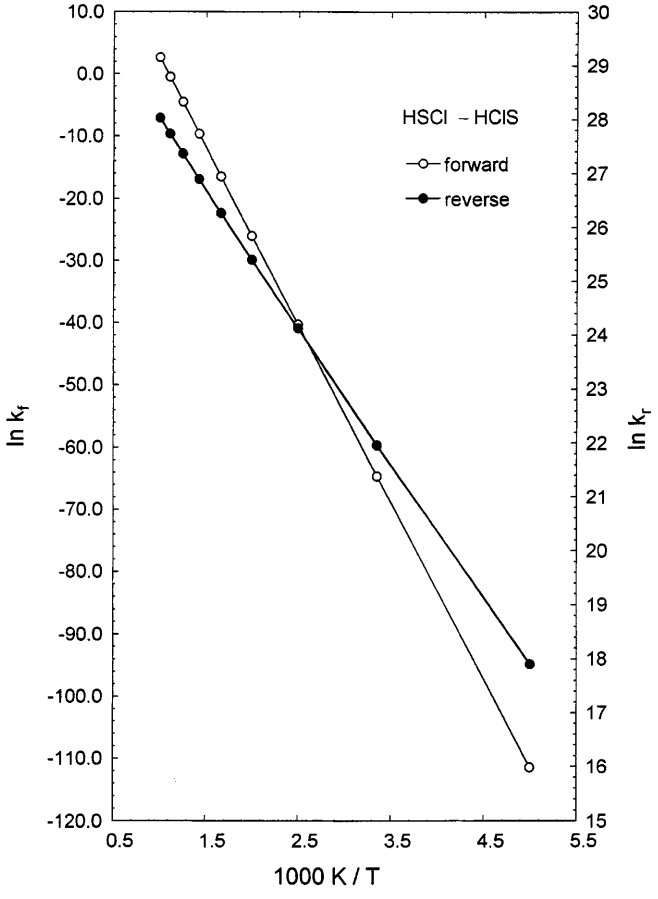

Fig. 4. Linear Arrhenius plot of the rate constants for the HSCl → HClS reaction. Energetic data underlying the calculation of the rate constant were computed with the coupled-cluster technique with all single and double excitations and connected triples and the correlation-consistent polarized valence triple zeta basis set

Table 7. Thermochemical and kinetics data for the HSCl ↔ HClS reaction. The *superscript* w stands for the tunneling correction for the forward (*f*) and reverse (*r*) reactions, and ‡ stands for the transition-state data

T (K)	ΔH^0 (kcal/mol)	$\Delta H^{0‡}$ (kcal/mol)	ΔG^0 (kcal/mol)	$\Delta G^{0‡}$ (kcal/mol)	k_f (s^{-1})	k_f^w (s^{-1})	k_r (s^{-1})	k_r^w (s^{-1})	K_e
200	51.52	55.96	51.41	55.85	3.91 (−49)	8.84 (−49)	5.95 (+7)	1.35 (+8)	6.57 (−57)
298.15	51.60	55.98	51.35	55.79	7.95 (−29)	1.25 (−28)	3.42 (+9)	5.40 (+9)	2.31 (−38)
400	51.67	55.95	51.25	55.73	2.98 (−18)	3.92 (−18)	2.96 (+10)	3.92 (+10)	1.00 (−28)
500	51.73	55.87	51.13	55.68	4.80 (−12)	5.77 (−12)	1.07 (+11)	1.29 (+11)	4.47 (−21)
600	51.77	55.76	51.01	55.65	6.71 (−8)	7.65 (−8)	2.54 (+11)	2.91 (+11)	2.63 (−19)
700	51.80	55.64	50.88	55.64	6.20 (−5)	6.84 (−5)	4.75 (+11)	5.25 (+11)	1.30 (−16)
800	51.83	55.50	50.75	55.65	1.04 (−2)	1.89 (−2)	7.61 (+11)	1.38 (+12)	1.37 (−14)
900	51.84	55.35	50.61	55.68	5.66 (−1)	6.01 (−1)	1.10 (+12)	1.17 (+12)	5.13 (−13)
1000	51.85	55.19	50.47	55.72	1.38 (+1)	1.45 (+1)	1.48 (+12)	1.56 (+12)	9.32 (−12)

Table 8. Arrhenius equation parameters for the HSCl → HClS reaction for several temperature intervals

Temperature interval	E_a (kcal/mol)	A (s^{-1})
200 – 298.15	56.46	1.91×10^{13}
298.15 – 400	56.65	2.67×10^{13}
400 – 500	56.80	3.23×10^{13}
500 – 600	56.90	3.58×10^{13}
600 – 700	57.00	3.87×10^{13}
700 – 800	57.00	4.87×10^{13}
800 – 900	57.19	4.36×10^{13}
900 – 1000	57.13	4.21×10^{13}

factor of 1.57 at 298.15 K, which then decreases with increasing temperatures, reaching a value of 1.05 at 1000 K. An Arrhenius linear fit to the rate constants is shown in Fig. 4, and values for the activation energy and the constant A, determined by a two-points fit to the Arrhenius equation, for several temperature intervals, are collected in Table 8 for the forward and reverse reactions.

4 Conclusions

Stationary points on the [H,S,Cl] PES have been located corresponding to a very stable HSCl species, to an isomer HClS, 51.84 kcal/mol higher in energy, and to a transition-state species, at 57.68 kcal/mol above HSCl, at the CCSD(T)/cc-pVTZ level of theory. The effects of different methods and basis sets were systematically investigated, indicating the reliability of the results, in particular, those with the smaller 6-31G(d,p) basis, which turned out to be poor for the HClS species. Vibrational frequencies data allow a clear differentiation between the two species to be made. Bonding differences were also discussed and illustrated by density contour plots of the valence orbitals. A Mulliken population analysis predicted a charge migration towards the S atom in HClS. Rate constants, within the TST and equilibrium constants for the HSCl ↔ HClS isomerization reaction were estimated for temperatures in the range 200–1000 K. At 298.15 K, the forward rate is predicted to be 7.95×10^{-29} s^{-1}, and the equilibrium constant to be 2.31×10^{-38}. Tunneling corrections to the rates change from 1.57 at 298.15 K to 1.05 at 1000 K. In the temperature range 298.15–400 K, the activation energy turned out to be 56.65 kcal/mol and the A factor to be 2.67×10^{13} s^{-1}.

Acknowledgements. The author is grateful to FAPESP and CNPq for continuous academic support, and to the Laboratório de Computação Científica Avançada, of the University of São Paulo, for the provision of computational facilities and technical support.

References

1. Wayne RP (1991) Chemistry of the atmospheres. Clarendon, Oxford
2. Eberhard J, Chen WC, Yu CH, Lee YP, Cheng BM (1998) J Chem Phys 108: 6197
3. Frisch MJ, Trucks GW, Schlegel HB, Gill PMW, Johnson BG, Robb MA, Cheeseman JR, Keith T, Petersson GA, Montgomery JA, Raghavachari K, Al-Laham MA, Zakrzewski VG, Ortiz JV, Foresman JB, Cioslowski J, Stefanov BB, Nanayakkara A, Challacombe M, Peng CY, Ayala PY, Chen W, Wong MW, Andres JL, Replogle ES, Gomperts R, Martin RL, Fox DJ, Binkley JS, Defrees DJ, Baker J, Stewart JP, Head-Gordon M, Gonzalez C, Pople JA (1995) Gaussian 94, revision D.2. Gaussian, Pittsburgh, Pa
4. (a) Hariharan PC, Pople JA (1973) Theor Chim Acta 28: 213; (b) Hehre WJ, Ditchfield R, Pople JA (1972) J Chem Phys 56: 2257; (c) Ditchfield R, Hehre WJ, Pople JA (1971) J Chem Phys 54: 724
5. (a) Dunning TH (1989) J Chem Phys 90: 1007; (b) Kendall RA, Dunning TH, Harrison RJ (1992) J Chem Phys 96: 6796; (c) Woon DE, Dunning TH (1993) J Chem Phys 98: 1358
6. Glasstone S, Laidler K, Eyring H (1941) The theory of rate processes. Mc Graw-Hill, New York
7. Wigner EP (1932) Z Phys Chem Abt B 19: 203
8. Yamada C, Butler JE, Kawaguchi K, Kanamori H, Hirota E (1986) J Mol Spectrosc 116: 108
9. Huber KP, Herzberg G (1979) Molecular spectra and molecular structure, vol IV. Constants of diatomic molecules. Van Nostrand Reinhold, New York
10. (a) Gonzales C, Schlegel HB (1990) J Phys Chem 94: 5523; (b) Gonzales C, Schlegel HB (1990) J Phys Chem 90: 2154
11. Chase MW, Davies CA, Downey JR, Frurip DJ, McDonald RA, Syverud AN (1985) J Phys Chem Ref Data 14: Suppl 1–2
12. Gerhold G, McMurchie L, Tye T (1972) Am J Phys 40: 988
13. Davidson ER, Langhoff SR, Elbert ST, McMurchie LE, with subsequent extensive modifications by Feller D, Rawlings DC MELD
14. Lee TJ, Taylor PR (1989) Int J Quantum Chem Symp 23: 199